Photoluminescence above the Tauc gap in a-Si:H

I. H. Campbell, P. M. Fauchet, and S. A. Lyon
Department of Electrical Engineering and Advanced Technology Center for Photonic and Opto-electronic Materials, Princeton University, Princeton, New Jersey 08544

R. J. Nemanich
Department of Physics, North Carolina State University, Raleigh, North Carolina 27695
(Received 27 September 1989)

We report the observation of photoluminescence (PL) significantly above the Tauc gap in a-Si:H. The dependence on temperature, incident intensity, excitation energy, deep-defect concentration, and time-resolved measurements are presented. The PL begins at the excitation energy, decreases in intensity as the photon energy decreases, reaches at a minimum at ~2 eV, and then increases exponentially until it approaches the PL peak at 1.4 eV. The luminescence above ~2 eV is weak and temperature independent. It is attributed to the recombination of nonthermal electrons with nonthermal holes. Below ~2 eV, the luminescence depends on temperature and deep-defect density. It results from the recombination of electrons and holes in the band tails. At low temperature, the slope of the luminescence indicates that the radius of the electron wave function in the band tail is ~10 Å.

I. INTRODUCTION

Photoluminescence (PL) in a-Si:H has been studied extensively by many workers and was reviewed recently by Street.[1] Most of the previous studies have been concerned with the luminescence peak in a-Si:H that occurs at ~1.4 eV at 10 K. This peak is strongest in samples with a low density of deep defects and is attributed to carriers trapped in the conduction- and valence-band tails. At this time there is no generally agreed upon model that quantitatively explains the spectral form of this luminescence. It has been proposed that the luminescence is the result of recombination by either geminate pairs,[1] nongeminate distant pairs,[2] or excitons.[3,4] The extent to which phonon interactions determine the energy of the PL is still unresolved; Street argues for a Stokes shift of up to 0.5 eV, while Boulitrop argues for an insignificant lattice relaxation. The long carrier lifetimes in the band tails allow a large steady-state population to be created and it appears that the peak luminescence is linear with intensity (geminate) only at very low intensities ~1 mW/cm^2.

There have been few reports of higher-energy PL in a-Si:H. Shah[5] reported the observation of strong above-Tauc-gap PL in a-Si:H with a broad, temperature-independent peak that shifted with excitation energy. Wilson[6] demonstrated that the PL observed by Shah was due to surface contaminants commonly found in the laboratory environment and was not an intrinsic property of the material. Shah[7] measured the excitation-energy dependence of the PL and found that the spectral form of the luminescence was constant when excited with energies greater than 1.8 eV and below that there was a peak shift toward lower energy as the excitation energy was decreased. He interpreted this excitation-energy dependence by postulating a thermalization gap at 1.8 eV, above which the carriers lost energy nonradiatively and therefore had no memory of their initial state. Below 1.8 eV the carriers are created in band-tail states and nonradiative thermalization is restricted. He also observed that the high-energy tail of the luminescence, when excited with high-energy excitation, cut off sharply at 1.8 eV when plotted on a logarithmic scale. In fact, Shah could not detect any luminescence above ~1.8 eV. Orlowski[8] measured time-resolved PL with 2.33-eV excitation using a streak camera. He found that the luminescence extends to energies greater than 1.8 eV for times less than 100 ps after excitation, but he was unable to spectrally resolve the high-energy PL.

We report the observation of above-Tauc-gap PL in a-Si:H that becomes significant at approximately 2 eV and then increases exponentially with decreasing photon energy. This luminescence is the high-energy tail of the commonly observed 1.4-eV luminescence peak. We have measured its dependence on temperature, intensity, deep-defect density, and excitation energy. At and above room temperature, this high-energy tail results from thermal electrons recombining with self-trapped holes, while below 300 K it is due to recombination of nonthermal electrons and trapped holes. The slope of the high-energy tail can be used to estimate the radius of the electron wave function in the band tail. In addition, we have also measured weak, temperature-independent luminescence above 2 eV that increases with increasing photon energy. We attribute this luminescence to geminate recombination of nonthermal carriers in the extended states. This weak PL provides information about the energy-loss rate, radiative lifetime, and mobility of the excited carriers.

II. EXPERIMENT

The *a*-Si:H films were prepared by either rf or dc glow discharge and varied in thickness from 0.1 to 5 μm. The films were deposited on fused-quartz substrates and also on crystalline Si for low-temperature luminescence experiments. The films were deposited on crystalline substrates in order to prevent laser-induced sample heating, which is significant for fused-quartz substrates below $\sim$200 K. The luminescence spectra were obtained using either the 457-, 488-, or 514-nm, lines of a cw Ar^+ laser or the 578-nm line of a copper-vapor laser producing 20-ns pulses at 8.8 kHz. The intensity was varied by more than an order of magnitude, but was typically $\sim$10 W/cm^2 for cw excitation and $\sim 10^6$ W/cm^2 for the pulsed excitation. The spectral response of the combined spectrometer and photomultiplier system was measured and is essentially uniform within the range of interest. To ensure that the weak luminescence near the laser line was not due to scattered light, the laser was operated in a single longitudinal mode tuned to an I_2 absorption line.[9] A temperature-controlled I_2 cell was placed in front of the spectrometer entrance slit to absorb the elastically scattered light. The attenuation of the elastically scattered light was controlled by the cell temperature, which changes the iodine vapor pressure. By acquiring spectra at two different cell temperatures, the contribution of the elastically scattered light was determined to be a negligible component of the luminescence. Using the I_2 cell and a triple spectrometer, it was possible to work within 10 cm^{-1} of the laser line.

III. RESULTS

A. cw results

The 2.41-eV excited luminescence spectrum of *a*-Si:H from 10 K to room temperature is shown in Fig. 1, and from room temperature to 500 K in Fig. 2 for a different sample. The luminescence initially decreases upon going from 2.3 to 2 eV, reaches a minimum at 2 eV (greater than the system dark count), and then increases exponentially from 2 to 1.55 eV. The second-order Si-Si Raman peak[10] at $\sim$950 cm^{-1} and the Si-H Raman peak[10] at $\sim$2000 cm^{-1} compete with the luminescence above 2 eV. There is, however, a clearly discernible luminescence contribution that decreases linearly with energy away from the excitation energy (compare with the crystalline-silicon spectrum shown in Fig. 7). We define the onset of the exponential luminescence, E_{on}, to be the intersection of the minimum luminescence and the exponentially in-

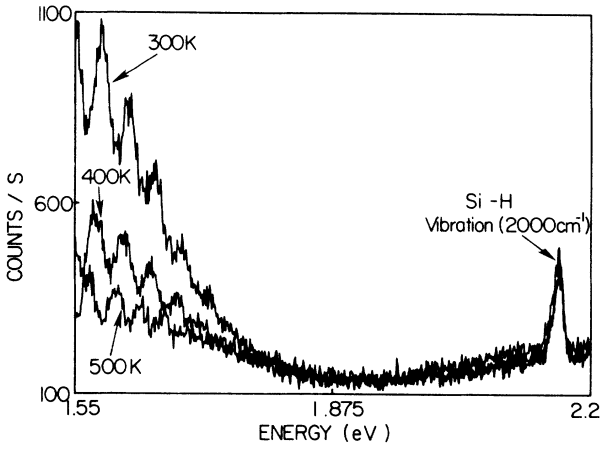

FIG. 2. Temperature dependence of the 2.41-eV excited luminescence of *a*-Si:H on a glass substrate from 300 to 500 K. Note the clearly observable interference fringes from 1.55 to 1.7 eV, below the Tauc gap. The energy scale is 0.1 eV smaller than in Fig. 1.

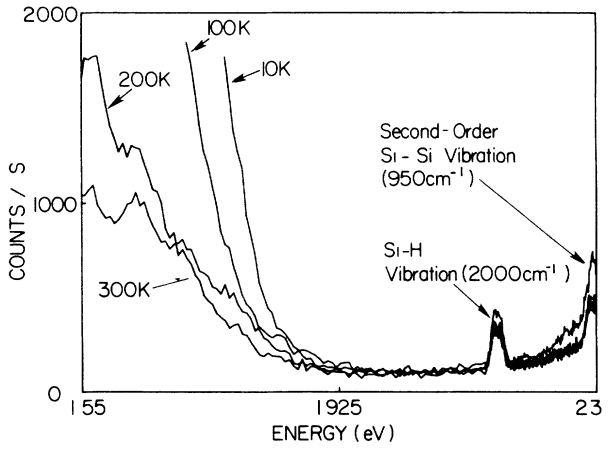

FIG. 1. Temperature dependence of the 2.41-eV excited luminescence of *a*-Si:H on a *c*-Si substrate from 10 to 300 K. Note the increase of the PL at higher energy and the Raman features at 2.15 and 2.29 eV. The PL minimum is much greater than the system dark count.

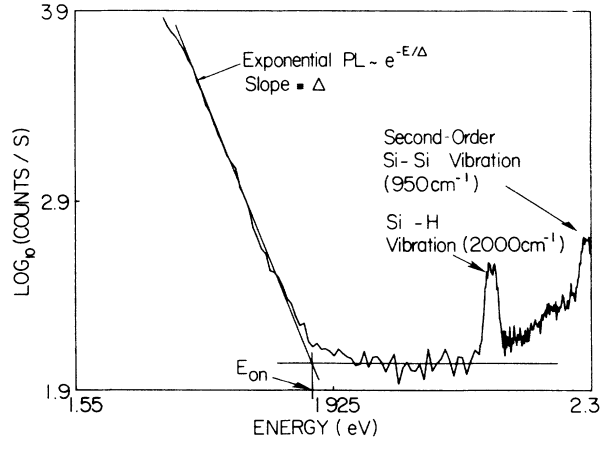

FIG. 3. Definition of the onset, E_{on}, and slope, Δ, of the cw luminescence. The slope is obtained by fitting the luminescence to the form $e^{-E/\Delta}$, and the onset is the intersection of the relatively constant luminescence around 2 eV and the extrapolation of the exponential luminescence.

creasing luminescence and the slope, Δ, to be determined by fitting the exponential luminescence to the form $\exp(-E/\Delta)$, as shown in Fig. 3. The luminescence intensity above E_{on} is temperature independent, but both the onset and slope of the exponential luminescence decrease as the temperature is lowered, as shown in Fig. 4. The onset of the exponential luminescence is nearly 2.0 eV at 300 K and decreases to ~ 1.88 eV at 100 K and lower. The slope decreases from 240 meV at 500 K to 50 meV at 10 K. The temperature dependence of the Tauc gap[11] and kT are also plotted in Fig. 4. Unlike the PL onset, the Tauc gap increases with decreasing temperature. This opposite temperature dependence implies that the PL onset is not simply associated with a particular region of the electronic density of states of the sample. The PL slope in amorphous silicon is greater than kT from 10 to 500 K, in contrast to crystalline semiconductors, in which the PL slope is $\sim kT$.[12] The room-temperature PL spectra of three samples with different deep-defect concentrations, N_s, are plotted in Fig. 5. The deep-defect density was measured either by the constant-photocurrent method or by photothermal deflection spectroscopy. The PL is strongest in the sample with the smallest N_s and is practically nonexistent for $N_s \gtrsim 10^{18}$ cm^{-3}.

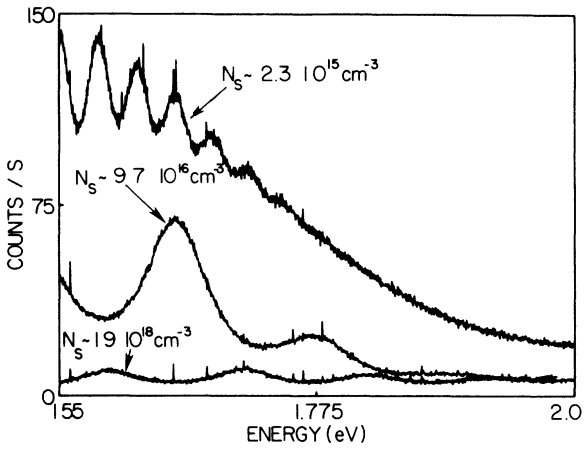

FIG. 5. Qualitative dependence of the room-temperature PL on the deep-defect density, N_s. As N_s increases, the luminescence is gradually suppressed. The samples all have approximately the same Tauc gap.

The intensity dependence of the luminescence at room temperature is shown in Fig. 6. The luminescence at energies $\geq E_{on}$ increases linearly with power at all measured intensities, while the exponential luminescence is linear at low power and then begins to saturate at $\sim 10^3$ W/cm^2 (not shown in Fig. 6). Figure 7 contains a luminescence spectrum of amorphous silicon and a reference spectrum of crystalline silicon showing the complete absence of any spurious luminescence above 1.5 eV. The

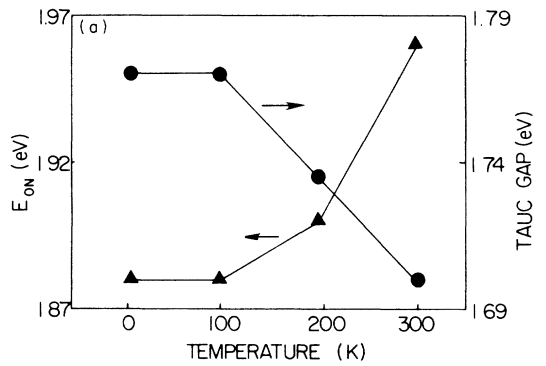

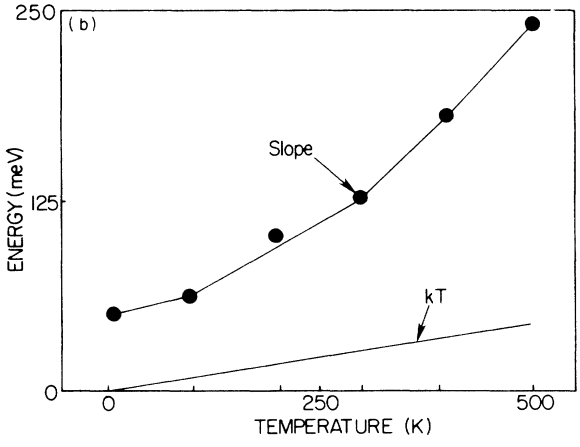

FIG. 4. (a) PL onset and sample Tauc gap (Ref. 11) as functions of temperature. The onset and Tauc gap have opposite temperature dependence. The lines are guides to the eye. (b) PL slope and kT as functions of temperature. The slope is always $\gg kT$, unlike crystalline semiconductors. The line is a guide to the eye.

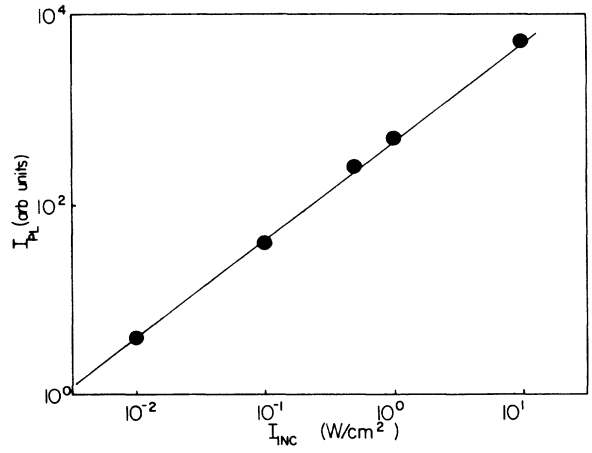

FIG. 6. Intensity dependence of the luminescence from $\sim 10^{-2}$ to 10 W/cm^2 at room temperature. Throughout the range of intensities shown, the PL above and below E_{on} increases linearly with intensity. A line with a slope of 1 is included for reference.

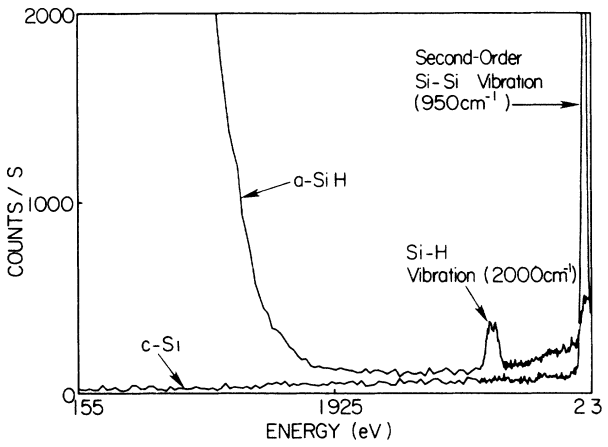

FIG. 7. PL spectra of *a*-Si:H and *c*-Si recorded under identical conditions. *c*-Si does not luminesce in this region, but has a sharp second-order Raman feature at 2.28 eV. The *c*-Si luminescence peak is at ~1.16 eV.

crystalline silicon peak is at ~1.16 eV.

In general, the PL below E_{on} was independent of excitation wavelength, but the PL above E_{on} was often partially obscured by both elastic and inelastic light scattering. We have chosen to present results obtained only with 2.41-eV excitation because the use of an I_2 cell enabled us to determine the effects of the elastically scattered light. Because of the absorption spectrum of I_2, we could not use the cell at wavelengths significantly different from 514 nm.

B. Time-resolved measurements

The results of time-resolved, room-temperature luminescence experiments are shown in Fig. 8. Since

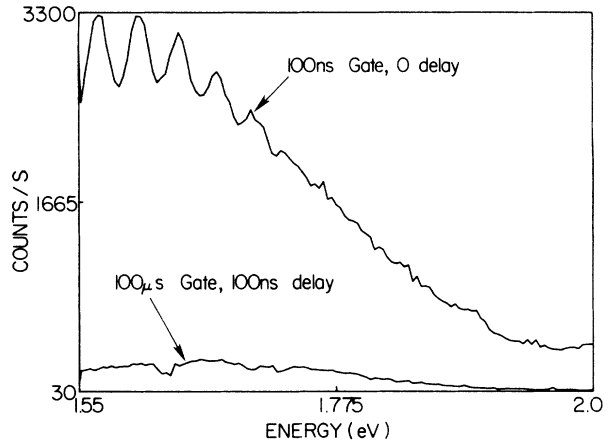

FIG. 8. Gated time-resolved PL using 2.15-eV, 10-ns pulse excitation. The upper trace was taken with a 100-ns gate and 0 delay between the gate and the excitation pulse. The lower curve was acquired with a 100-μs gate applied 100 ns after excitation.

2.15-eV excitation was used, only the luminescence below E_{on} was measured. The upper spectrum was acquired with a 100-ns gate applied immediately after excitation and the lower spectrum was taken with a 100-μs gate applied 100 ns after excitation. The two spectra are complementary in that the total luminescence emitted from the sample is simply the sum of the two curves. The time-resolved spectra are identical to the cw spectra and they indicate that at least 90% of the luminescence is emitted within the first 100 ns.

IV. MODELS

A. General considerations

All of the luminescence we report is linear with pump intensity over at least 1 order of magnitude. On the surface this seems to contradict the results of Street,[1] who found the luminescence to be linear with intensity (geminate) only at intensities below ~1 mW/cm^2, which is 4 orders of magnitude below the intensities we used. Also, the temperature dependence of the luminescence peak as measured by Collins[13] is not the same as that of the high-energy luminescence we observe. The differences between these measurements can be accounted for by the different spectral regions observed. Street and Collins were examining the peak of the Pl signal at 1.4 eV, while we are concerned with the 1.8-eV region around the Tauc gap. The carriers involved in the PL we observe are significantly less localized than those luminescing at 1.4 eV. We have verified that our samples do have a luminescence peak at approximately 1.4 eV, and that the exponential luminescence we observe is the high-energy tail of this peak and not part of a separate luminescence feature.

The exciting photon energies used in our experiments create electron and hole pairs high in the conduction and valence bands. After excitation, the carriers begin to lose energy to the lattice, eventually reaching thermal equilibrium with the lattice. For discussion purposes we define thermal electrons as electrons whose energy distribution can be described by a Fermi-Dirac distribution at the lattice temperature, while hot or nonthermal electrons cannot. We assume that carrier-carrier processes are insignificant compared to carrier-phonon interactions in determining the steady-state electron distribution, and therefore both hot and thermal electrons may exist simultaneously in the sample. We divide the luminescence into two distinct regions: one above and the other below E_{on}. The two regions seem to be of separate origin; they have different temperature and intensity dependence and there is a sharp demarcation between them.

B. Luminescence above E_{on}

Because of its high energy and temperature and intensity independence, we attribute the luminescence above E_{on} to geminate recombination of nonthermal carriers in the extended states. The dominant electron-hole transitions and approximate steady-state carrier distributions responsible for this luminescence are shown superimposed on the *a*-Si:H density of states in Fig. 9. Although

the dominant energy-loss mechanism for the hot carriers is phonon emission, some carriers recombine radiatively with their geminate partner. By measuring the absolute luminescence efficiency, we can extract the ratio of the nonradiative and radiative lifetimes since these processes occur in parallel. The luminescence near the excitation energy is entirely from hot electrons and hot holes, and so we consider the luminescence approximately 0.1 eV from the excitation. Our combined spectrometer throughput and photomultiplier response is approximately 1% (measured) and that of our collection optics is 1% (calculated including the index of refraction of the sample), and so our overall detection efficiency is 10^{-4}. We inject 10^{17} electrons and holes per second, and the integrated luminescence in a 50-meV window is 10^8 photons/s, including the overall efficiency. In our case, the radiative lifetime is much longer than the nonradiative lifetime, so the luminescence efficiency is

$$\frac{\tau_{\rm nr}}{\tau_r+\tau_{\rm nr}} \cong \frac{\tau_{\rm nr}}{\tau_r} = \frac{10^8}{10^{17}} = 10^{-9} . \tag{1}$$

If we further assume a nonradiative lifetime of 50 fs (i.e., the electron and hole each lose (50 meV)/(100 fs) and jointly occupy our chosen 50-meV window for 50 fs), then the effective radiative lifetime is $(5\times10^{-14}\ \text{s})/10^{-9} = 5\times10^{-5}$ s. If the electron and hole are overlapped in space and the transition is dipole allowed, then we would expect a radiative lifetime of ~ 10 ns. The increase in the radiative lifetime is due to the spatial separation of the carriers that have moved away from one another. To consider the effect of the carrier separation, we decompose the optical matrix element into two terms: an envelope matrix element that describes the spatial overlap of the carriers, and an atomic matrix element that represents the dipole matrix element for spatially overlapped carriers. The optical matrix element can be written as

$$M^2 \cong \left| \left\langle \Psi_h \left| \frac{\partial}{\partial r} \right| \Psi_e \right\rangle \right|^2 , \tag{2}$$

where $\Psi_{h\,(e)}$ is the hole (electron) wave function. Writing the electron or hole wave functions as the product of an envelope wave function and an atomic wave function, we have

$$\Psi_{h\,(e)} = \Psi^{\rm env}_{h\,(e)} \Psi^{\rm at}_{h\,(e)} , \tag{3}$$

where $\Psi^{\rm env\,(at)}_{h\,(e)}$ is the envelope (atomic) wave function for the hole (electron). The envelope wave function varies slowly in space compared to the atomic wave function, so we assume $(\partial/\partial r)\Psi^{\rm env}_{h\,(e)} = 0$, and write the final matrix element as

$$M^2 \cong |\langle \Psi^{\rm env}_h | \Psi^{\rm env}_e \rangle|^2 \left| \left\langle \Psi^{\rm at}_h \left| \frac{\partial}{\partial r} \right| \Psi^{\rm at}_e \right\rangle \right|^2$$
$$= M^2_{\rm env} M^2_{\rm at} . \tag{4}$$

The radiative lifetime is approximately 10 ns only if the electron and hole overlap in space, i.e., if $|\langle \Psi^{\rm env}_h | \Psi^{\rm env}_e \rangle| = 1$.

To calculate the luminescence from the diffusing electron and hole, we assume that the radius of the electron envelope is much larger than that of the hole ($r_e \gg r_h$), and further approximate the hole envelope as a hard sphere centered at the origin, i.e.,

$$|\Psi^{\rm env}_h|^2 = \frac{3}{4\pi r_h^3} \quad \text{for } 0 < r \le r_h . \tag{5}$$

We take the electron envelope to be centered at r_0 and to decay exponentially with radius r_e ($|\Psi^{\rm env}_e|^2$ has radius r_e), i.e.,

$$|\Psi^{\rm env}_e|^2 = \frac{1}{8\pi r_e^3} e^{-|r-r_0|/r_e} . \tag{6}$$

For a particle diffusing from the origin, the probability of finding it at a position r after a time t is given by[14]

$$p(r,t) = \frac{1}{\pi^{1/5} l^3} e^{-r^2/l^2} , \tag{7}$$

where $l = \sqrt{4Dt}$, and D is the diffusivity. Considering only electron diffusion, the envelope matrix element becomes

$$M^2_{\rm env} = \int_0^\infty 4\pi r_0^2 p(r_0,t) |\langle \Psi_h | \Psi_e(r_0) \rangle|^2 \, dr_0 . \tag{8}$$

We are interested in the decrease of the matrix element

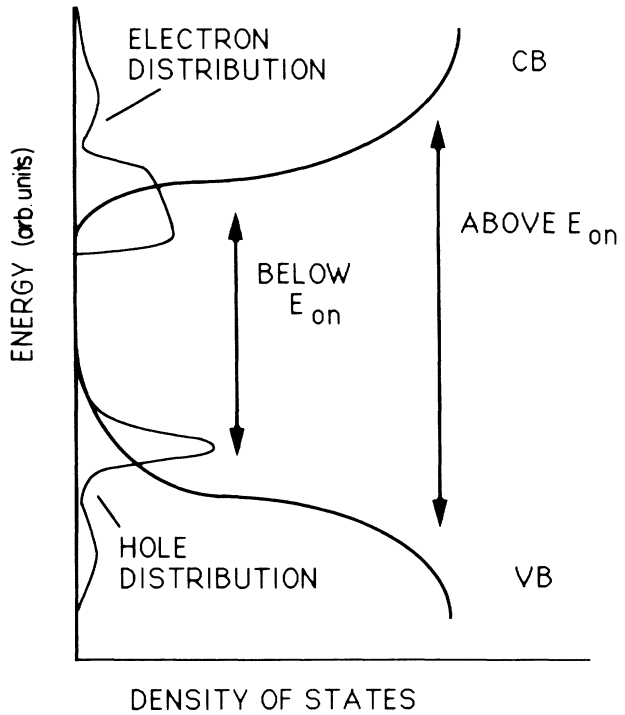

FIG. 9. Schematic representation of the *a*-Si:H density of states. The dominant luminescence transitions above and below $E_{\rm on}$ are indicated by the vertical lines. The approximate, steady-state electron and hole distributions indicate the trapped-hole population and the almost uniformly distributed electrons in the band tail.

due to diffusion, i.e., M^2/M_{at}^2, since $M^2=M_{at}^2$ at $t=0$. Neglecting higher-order terms, we have

$$\frac{M^2}{M_{at}^2}=\frac{8}{\sqrt{\pi}}\frac{r_e^3}{l^3} . \tag{9}$$

As M_{at}^2 leads to a radiative lifetime of 10^{-8} s, and the effective radiative lifetime is 5×10^{-5} s, it follows that $M^2/M_{at}^2=10^{-8}/(5\times10^{-5})\sim2\times10^{-4}$. The combined energy-loss rate of both carriers is ~1 eV/ps, so the diffusion time is ~100 fs. In order to fit our observed data, we either have to assume a diffusion coefficient for hot electrons or use an estimate of the electron wave function. Unfortunately, neither of these parameters are well known. If we assume an electron mobility of 6 cm^2/V (Ref. 15) and an effective electron temperature of 200 meV, this yields a diffusion coefficient of 1.2 cm^2/s [$D=(kT/q)\mu$]. This choice of diffusion coefficient implies that the electron diffuses 70 Å in the first 100 fs. If we try to fit our luminescence efficiency using this diffusion length, it requires that the radius of the electron wave function be 5 Å, and our simple model, in which we neglect the hole, is no longer valid. This radius, which is 3 times smaller than the inelastic diffusion length of an electron in the conduction band as determined by Mott,[16] is unphysically small for electrons in the extended states. In contrast, if we assume that the radius of the electron wave function is 30 Å ($r_e=15$ Å), this requires that the electron diffuses 425 Å in the first 100 fs. In this case our model no longer applies because the electron motion that this implies would be ballistic and not diffusive transport. Ballistic motion of electrons over hundreds of angstroms should not occur in amorphous silicon because of the intrinsic potential disorder. There are many uncertainties in the parameters used to fit the data. The radiative lifetime, nonradiative energy-loss rate, and electron mobility we use are plausible, but they may be in error by a factor of 2 or more. Unfortunately, it does not appear possible to fit our observed PL intensity using reasonable values of these parameters with the above model. At the present time it is not clear how to explain quantitatively the magnitude of this luminescence.

In the spectral region 2.1–2.3 eV we observe a linear increase in the luminescence signal with increasing photon energy. In the above model, this implies that the radiative recombination rate increases more rapidly as a function of energy than the nonradiative rate. The high-energy luminescence in this region is predominantly due to the recombination of carriers high in their respective bands, and increasing photon energy corresponds to increasing carrier energy. The radiative recombination rate increases with increasing carrier energy because the carriers are closer together (less diffusion time) and the nonradiative rate is independent of energy for these nonthermal carriers. In the above model the radiative rate, W_r, is proportional to l^{-3} with $l\propto t^{1/2}$ (diffusion). We assumed a constant energy-loss rate, so we can write the energy of the carrier in the band as $E=E_0-ct$, where E_0 is the energy of the carrier in the band immediately after excitation and c is the energy-independent energy-loss rate. The radiative rate becomes

$$W_r\propto l^{-3}\propto(1-E/E_0)^{-3/2} . \tag{10}$$

Assuming that $E_0>E$, then $W_r\propto E$, which is consistent with the linear increase in PL signal that we observe. If the energy-loss rate was increasing as the square root of the carrier energy (proportional to the velocity) for each carrier,[17] then the luminescence signal would increase sublinearly with photon energy in this range.

C. Luminescence below E_{on}

The energy of the exponential PL, its continuity with the main luminescence peak at 1.4 eV, and its decrease with increasing N_s indicate that, like the peak at 1.4 eV, it is due to carriers in the band-tail states. In addition, the temperature dependence of E_{on} above 200 K is only consistent with luminescence involving thermal carriers. E_{on} increases with temperature since the thermal-electron population shifts to higher energy with increasing temperature. If the PL above 200 K was from nonthermal carriers, then E_{on} should decrease with increasing temperature, following the temperature dependence of the Tauc gap. The magnitude of the exponential PL slope at temperatures above 200 K indicates that the luminescence below E_{on} is not analogous to band-to-band PL from thermal carriers in crystalline semiconductors [note that we use "PL slope" to refer to the denominator of the argument of the exponential in expressions describing the luminescence, i.e., for PL $\propto\exp(-E/\Delta)$, Δ is the slope]. In a crystalline semiconductor the PL slope is kT, determined only by the carrier distribution function because the density of states is not a strong function of energy compared to a Boltzmann distribution.[12] The PL slope we observe is much greater than that expected for extended-state to extended-state PL in a-Si:H. This suggests that the carriers occupy band-tail states since the energy dependence of the band-tail density of states (DOS) is significant compared to a high-temperature electron distribution and the energy dependence of the band-tail DOS acts to increase the slope. At temperatures below 200 K, however, the energy dependence of the band-tail density of states is insignificant compared to the electron distribution function and thermal carriers would lead to PL slopes comparable to kT. Since we observe a large slope, nonthermal carriers are most likely involved in the low-temperature PL. Based on time-of-flight[18] (TOF) and previous PL results[3,4] the high-temperature regime should be explained by a multiple-trapping process (thermal carriers) and the low-temperature results by hopping within the band tails (nonthermal carriers).

1. From room temperature to 500 K

The high-temperature luminescence (>200 K) should be explained using the multiple-trapping model of Tiedje and Rose[19] to calculate the electron and hole distributions in the band tails. For cw excitation multiple trapping is indistinguishable from simply assuming that the carrier distribution can be described using a Fermi-Dirac distribution at the lattice temperature.

Unfortunately, a straightforward application of the multiple-trapping model fails to accurately predict the

slope of the cw excited luminescence. Assuming a constant dipole matrix element between states in the two bands,[20] the luminescence rate can be written as

$$W_L(\hbar\omega) \propto \omega \int_0^{\hbar\omega} dE_c\, n(E_c) p(E_n \simeq \hbar\omega - E_c) , \quad (11)$$

where $\hbar\omega$ is the photon energy, $n(E_c)$ $[p(E_v)]$ is the number of electrons (holes) per unit energy in the conduction- (valence-) band tail, and $E_{c\,(v)}$ is the energy of the electron (hole) in the conduction (valence) band. In a-Si:H the electron (hole) band-tail density of states is exponential $\propto \exp(E_{c\,(v)}/E_{0c\,(0v)})$, where $E_{0c\,(0v)}$ is the slope of the conduction- (valence-) band-tail density of states. Assuming a Boltzmann distribution for the carriers, the number of electrons in the conduction-band tail per unit energy is

$$n(E_c) \propto \exp(E_c/E_{0c}) \exp(-E_c/kT) , \quad (12)$$

where T is the lattice temperature. A similar term applies to the holes in the valence-band tail. The luminescence is the difference of two exponential terms,

$$W_L(\hbar\omega) \propto \omega \frac{(E_{0c}E_{0v})}{(E_{0v}-E_{0c})} [\exp(-\hbar\omega/\Delta_c) - \exp(-\hbar\omega/\Delta_v)] , \quad (13)$$

where the slopes of the two luminescence terms are $\Delta_{c\,(v)} = E_{0c\,(0v)} kT/(E_{0c\,(0v)} - kT)$, which come from the product of the exponential density of states and the Boltzmann distribution function in Eq. (12). The slope of the valence-band-tail density of states is larger than that of the conduction-band-tail density of states, so the slope of the luminescence would be given by Δ_v (since $\Delta_c \gg \Delta_v$). This would yield a slope of 50 meV at room temperature, which is much steeper than the observed slope of ~ 120 meV.

Nevertheless, it is difficult to conceive that the carriers responsible for the luminescence below E_{on} are not thermal. The temperature dependence of the PL onset and slope, the decrease in PL intensity with increasing N_s, and the continuity of the high-energy PL with the peak at 1.4 eV imply that the luminescence is from thermal carriers in the band tails.

In order to fit the observed slope of the luminescence, it is simplest to continue to assume that the electrons can be described by a Boltzmann distribution and that, instead of being thermally distributed, the holes have become self-trapped and are primarily located in a small energy range.[21] The dominant electron-hole transitions and approximate steady-state carrier distributions responsible for this luminescence are shown superimposed on the a-Si:H density of states in Fig. 9. In steady state one expects the larger valence-band-tail DOS and effective mass to lead to significantly more self-trapped holes than electrons. For our pulsed measurements there is sufficient time (> 10 ns) for the lattice to distort and trap the hole,[22] consistent with the equivalence of the pulsed and cw measurements. By making these assumptions, the luminescence becomes

$$W_L(\hbar\omega) \propto \omega[\exp(-\hbar\omega/\Delta_c)] . \quad (14)$$

As shown in Table I, this expression yields reasonable agreement with the observed luminescence slopes in the temperature range 300–500 K over which the multiple-trapping model is expected to apply. The conduction-band-tail slope used at 300 K was measured using the TOF technique and is typical[18] of a-Si:H, and the temperature dependence is similar to that observed for the more easily measured valence-band tail.[23] The luminescence slope is only consistent with trapped holes and not trapped electrons, because if we assume the holes are thermalized and the electrons are distributed in a narrow range of energy (as in the exciton model proposed by Kivelson and Gelatt[24]), the slope would be 50 meV at 300 K, which is much smaller than that observed. The slope of the luminescence is, however, extremely sensitive to both the conduction-band-tail slope and the temperature; for example, if we assume the conduction-band-tail slope is 30 meV instead of 33 meV, then the slope changes from 120 to 189 meV, or if we assume a laser-induced temperature rise of 30 K, then the slope becomes 208 meV. The slope is extremely sensitive to these parameters because it depends on the product of two exponentials with similar magnitudes of opposite sign. In contrast, if we had continued to assume that both electrons and holes were thermally distributed, then the luminescence slope would be relatively insensitive to small changes in the temperature and valence-band-tail slope.

In this model the luminescence intensity is linear with excitation because a steady-state population of trapped holes is created independent of excitation, and only the number of electrons in the band tail varies with excitation intensity. The steady-state-hole density is excitation independent because the self-trapped-hole lifetime is long enough that for all experimental intensities the trapped-hole population rapidly saturates. The electrons, required by charge neutrality to balance the trapped holes, presumably occupy deep states in the gap and do not contribute to the high-energy luminescence. At high intensity it should be possible to observe luminescence from holes higher in the band tail than the trapped holes, but other density-dependent recombination mechanisms may compete with luminescence at higher carrier densities. Femtosecond time-resolved measurements indicate a rapid ($\tau < 10$ ps) decrease in carrier density[25,26] in the

TABLE I. Calculated and measured luminescence slopes as a function of temperature from 300 to 500 K. The slopes are calculated using the temperature-dependent conduction-band-tail slopes (Refs. 17 and 22) as indicated.

	Calculated and measured luminescence slopes			
T (K)	E_{0c} (meV)	E_{0v} (meV)	Calc. slope (meV)	Meas. slope (meV)
300	25	48	122	127
400	34	57	181	178
500	43	66	253	243

10^{21}–10^{19}-cm^{-3} range unaccompanied by significant high-energy luminescence.[15]

To attempt to confirm that the luminescence below the exponential onset was coming from the band tails, we performed time-resolved luminescence measurements. As seen in Fig. 8, at least 90% of the luminescence is emitted in the first 100 ns, and the remaining 100 μs (our pulse separation) accounts for, at most, 10% of the luminescence. This agrees with the transient-photocurrent results of Hvam[27] performed on intrinsic a-Si:H at high injection densities, $\gtrsim 10^{18}$ cm^{-3}. The luminescence results are essentially identical to the photocurrent results because nonradiative processes determine the electron dynamics in each case. Our results are not comparable to TOF results because we inject a high density of carriers that are not rapidly separated by the applied electric field, as in TOF measurements. Our time-resolved measurements are consistent with recombination involving thermal electrons in the conduction-band tail, but it is difficult to distinguish between thermal and nonthermal electrons with nanosecond time resolution.

2. *From 6 to 200 K*

Below about 200 K the multiple-trapping model no longer applies to amorphous silicon. At these temperatures the reexcitation rate from the band tails to the extended states becomes long compared to the intraband-tail hopping from tail state to tail state. Therefore, to explain our results at low temperature, we invoke hopping in the band tails. We assume that the luminescence is the result of recombination from electrons and self-trapped holes similar to our room-temperature model, except that the electrons are not thermal. As before, the slope of the luminescence is approximately the slope of the electron population in the conduction-band tails. Since the electrons lose energy with time, we can write a simple steady-state equation requiring that the total rate into a level with energy E_c from all levels above it must be equal to the integrated rate out of the level to all levels below it, i.e.,

$$\int_{E_c}^{\infty} dE \frac{n(E)}{\tau(E_c)} = \int_{-\infty}^{E_c} dE \frac{n(E_c)}{\tau(E)} , \tag{15}$$

where we define $\tau(E_c)=e^{-E_c/\Gamma}$ as the lifetime connecting electronic states with energy E_c to those with energy greater than E_c. We choose the lifetime to be independent of the higher-energy state since the hopping rate is controlled by the state with the smaller density and wave function, which is the state with lower energy in the band tail. We solve Eq. (15) by requiring that the electron distribution in the conduction-band tail is $n(E_c)=e^{-E_c/\Delta}$, where Δ is the observed low-temperature luminescence slope. This implies that $\Gamma=\Delta$. Using this semiempirical determination of the energy dependence of the electron lifetime high in the band tail, we can obtain an approximate radius for the electron wave function. Following Monroe,[28] the hopping rate out of a state with energy E_c to all levels with lower energy is

$$\nu(E_c)=\nu_0 \exp[-2\gamma(N_{\mathrm{CBT}})^{-1/3}\exp(-E_c/3E_{0c})] , \tag{16}$$

where $1/\gamma$ is the radius of the wave function and N_{CBT} is the total number of conduction-band-tail (CBT) states. To convert our calculated lifetime, $\tau(E_c)$, to a total rate from a state with energy E_c to all states below it, we sum the rates to all levels below E_c weighted by the density of states, i.e.,

$$\nu(E_c)=\int_{-\infty}^{E_c} \frac{dE}{\tau(E)} \exp(E/E_{0c}) \cong \exp[E_c(1/\Delta+1/E_{0c})] . \tag{17}$$

Equating (16) and (17) and neglecting higher-order terms, we obtain

$$3E_{0c}/[2\gamma(N_{\mathrm{CBT}})^{-1/3}]=1/(1/\Delta+1/E_{0c}) . \tag{18}$$

Using a conduction-band-tail slope[18,23] of 20 meV at 6 K and an integrated band-tail density[18] of 10^{20} states/cm^{-3}, one obtains 10 Å for the radius of the electron wave function ($1/\gamma$) near the top of the band tail, where our measurement is made.

V. DISCUSSION

A. Luminescence above E_{on}

The luminescence above E_{on} is certainly geminate recombination of nonthermal carriers. Nongeminate recombination of nonthermal carriers does not occur because the effective joint density of electrons and holes separated by >2 eV is very small ($<10^{12}$ cm^{-3}), and so the average separation between them is large (>6000 Å). Nongeminate recombination involving a thermal band-tail carrier would necessarily involve a very energetic partner, of which there are very few, and so the process would be exceedingly weak.

The most interesting aspect of the luminescence above E_{on} is its relatively low intensity, which is difficult to explain with physically reasonable values for the nonradiative energy-loss rate, electron mobility, and wave-function-envelope radius.

B. Luminescence below E_{on}

Below 2 eV the explanation is more uncertain. The only real evidence that the holes are trapped and the electrons thermally distributed comes from the slope of the luminescence at and above room temperature. The slope of the luminescence is very sensitive to our chosen parameters, but, encouragingly, the slope is, if anything, larger than 120 meV (indicating a smaller conduction-band-tail slope) at room temperature, which is only consistent with thermal electrons. In highly defective samples the slope becomes very large, but this is because the electrons are being trapped in deep states before they luminesce.

The explanation of our low-temperature results is an extrapolation of the room-temperature explanation. The extrapolation is made plausible, however, by the time-resolved, low-temperature PL observed by Wilson.[3,4]

Wilson's measurements indicate that only one carrier is thermalizing, which is exactly what we would predict based on the recombination of electrons with metastable trapped holes.

VI. CONCLUSIONS

We report our measurements of cw and pulsed luminescence above the Tauc gap in amorphous hydrogenated silicon from 6 to 500 K. The luminescence above 2 eV results from geminate recombination of nonthermal electrons and holes. The exponential luminescence below 2 eV is the high-energy tail of the commonly observed band-tail to band-tail PL. Based on our measurements at and above room temperature, we propose that this high-energy tail is due to the recombination of thermal electrons with self-trapped holes. The PL slope implies that the radius of the electron wave function in the band tail is ~ 10 Å.

ACKNOWLEDGMENTS

This research was supported in part by Coherent, Inc., by Newport Corporation and by the U.S. National Science Foundation through Grant No. ESC-86-57263. One of us (P.M.F.) is also supported by the Alfred P. Sloan Foundation.

[1]R. A. Street, in *Semiconductors and Semimetals,* edited by Jacques I. Pankove (Academic, New York, 1984), Vol. 21, Pt. b, Chap. 7.
[2]F. Boulitrop and D. J. Dunstan, Phys. Rev. B **28**, 5923 (1982).
[3]B. A. Wilson, in *Tetrahedrally Bonded Amorphous Semiconductors,* edited by D. Adler and H. Fritzsche (Plenum, New York, 1985), p. 397.
[4]B. A. Wilson, T. P. Kerwin, and J. P. Harbison, Phys. Rev. B **31**, 7953 (1985).
[5]J. Shah, Solid State Commun. **36**, 195 (1980).
[6]B. A. Wilson, Phys. Rev. B **23**, 3102 (1981).
[7]J. Shah, A. Pinczuk, F. B. Alexander, and B. G. Bagley, Solid State Commun. **42**, 717 (1982).
[8]T. E. Orlowski and H. Scher, Phys. Rev. Lett. **54**, 220 (1985).
[9]G. E. Devlin, J. L. Davis, L. Chase, and S. Geshwind, Appl. Phys. Lett. **19**, 138 (1971).
[10]J. S. Lannin, in *Semiconductors and Semimetals* (Ref. 1), Vol. 21, Pt. b, Chap. 6.
[11]N. M. Ravinda and J. Narayan, J. Appl. Phys. **60**, 1139 (1986).
[12]S. A. Lyon, J. Lumin. **35**, 121 (1986).
[13]R. W. Collins and W. Paul, Phys. Rev. B **25**, 5257 (1982).
[14]H. S. Carslaw and J. C. Jaeger, *Conduction of Heat in Solids* (Oxford University Press, Oxford, 1984), p. 257.
[15]A. Mourchid, D. Hulin, C. Tanguy, R. Vanderhagen, and P. M. Fauchet, J. Non-Cryst. Solids (to be published).
[16]N. F. Mott, Philos. Mag. B **58**, 369 (1988).
[17]K. Seeger, *Semiconductor Physics* (Springer-Verlag, New York, 1985), Chap. 6.
[18]T. Tiedje, in *Semiconductors and Semimetals* (Ref. 1), Vol. 21, Pt. c, Chap. 6.
[19]T. Tiedje and A. Rose, Solid State Commun. **37**, 49 (1980).
[20]W. B. Jackson, S. M. Kelso, C. C. Tsai, J. W. Allen, and S.-J. Oh, Phys. Rev. B **31**, 5187 (1985).
[21]D. Emin, in *Electronic and Structural Properties of Amorphous Semiconductors,* edited by P. G Le Comber and J. Mort (Academic, London, 1973), p. 261.
[22]D. Emin, J. Non-Cryst. Solids **35&36**, 969 (1980).
[23]G. D. Cody, T. Tiedje, B. Abelès, B. Brooks, and Y. Goldstein, Phys. Rev. Lett. **47**, 1480 (1981).
[24]S. Kivelson and C. D. Gelatt, Jr., Phys. Rev. B **26**, 4646 (1982).
[25]P. M. Fauchet, D. Hulin, A. Migus, A. Antonetti, J. Kolodzey, and S. Wagner, Phys. Rev. Lett. **57**, 2438 (1986).
[26]C. Tanguy, D. Hulin, A. Mourchid, P. M. Fauchet, and S. Wagner, Appl. Phys. Lett. **53**, 880 (1988).
[27]J. M. Hvam and M. H. Brodsky, J. Phys. (Paris) Colloq. **42**, C4-551 (1981).
[28]D. Monroe, Phys. Rev. Lett. **54**, 146 (1985).